IL NUOVO CIMENTO Vol. 36 C, N. 1 Suppl. 1 Gennaio-Febbraio 2013
DOI 10.1393/ncc/i2013-11480-y

Colloquia: 12th Italian-Korean Symposium 2011

Neutron stars within a general relativistic theory including strong, weak and electromagnetic interactions

R. Belvedere([1])([2])(*), J. Rueda([1])([2])(**) and R. Ruffini([1])([2])(***)

([1]) *Dipartimento di Fisica, Sapienza Università di Roma, ICRA-International Center for Relativistic Astrophysics - P.le Aldo Moro 5, Rome, 00185, Italy*
([2]) *ICRANet - P.zza della Repubblica 10, Pescara, 65122, Italy*

ricevuto il 9 Marzo 2012

Summary. — We construct the ground-state equilibrium configurations of neutron stars. The system of equilibrium equations is obtained taking into account quantum statistics, electro-weak, and strong interactions, within the framework of general relativity in the non-rotating spherically symmetric case. The core is assumed to be composed of interacting degenerate neutrons, protons and electrons in beta equilibrium. The strong interaction between nucleons is modeled through sigma-omega-rho meson exchange model. The mass-radius relation for neutron star cores is obtained for the various nuclear parametrizations. The mass and the thickness of the outer crusts corresponding to the different core mass-radius relations are obtained. The analysis is performed for two selected equations of state (EoS)of the outer crust matter. The first one neglects the Coulomb interactions between the degenerate electrons and the nuclear component of fixed charge to mass ratio Z/A. The second EoS, takes into account the Coulomb interactions of the point-like nuclei with a uniform fluid of degenerate electrons and the nuclear contribution is obtained from experimental data of nuclear masses. The mass and the thickness of the outer crust obtained with these two different EoS are compared and contrasted. We obtain systematically outer crusts with smaller mass and larger thickness when Coulomb interactions are taken into account.

PACS 04.40.-b – Self-gravitating systems; continuous media and classical fields in curved spacetime.
PACS 97.60.Jd – Neutron stars.
PACS 26.60.-c – Nuclear matter aspects of neutron stars.
PACS 12.40.-y – Other models for strong interactions.

(*) E-mail: riccardo.belvedere@icra.it
(**) E-mail: jorge.rueda@icra.it
(***) E-mail: ruffini@icra.it

1. – Introduction

Neglecting any external field, thermodynamic equilibrium requires the constancy of both temperature and particle chemical potential throughout the whole configuration. Introducing an external field, the latter condition becomes $\mu_0 + U = \text{const}$ [1], where U denotes the external potential and μ_0 is the "free" particle chemical potential. O. Klein, investigating the thermodynamic equilibrium conditions of a self-gravitating one-component fluid of non-interacting neutral particles in spherical symmetry, extended these equilibrium condition to the case of general relativity [2]. Further steps were made first by T. Kodama and M. Yamada [3], generalizing the Klein's equilibrium conditions to the case of a multicomponent fluid of non-interacting neutral particles, then by E. Olson and M. Bailyn [4], which described the case of a self-gravitating multicomponent fluid of charged particles taking into account the Coulomb interaction. The generalization of all the above works to the case of strong interactions, has been recently accomplished in [5], for a system of neutrons, protons and electrons in beta equilibrium. A general relativistic Thomas-Fermi treatment of nuclear matter within the framework of quantum statistics and of the general relativistic field theory for the gravitational, the electromagnetic and the hadronic fields, has been there constructed. The constancy of the general relativistic Fermi energy of particles

$$E_n^F = \sqrt{g_{00}}\mu_n + g_\omega\omega - g_\rho\rho, \tag{1}$$

$$E_p^F = \sqrt{g_{00}}\mu_p + g_\omega\omega + g_\rho\rho + eV, \tag{2}$$

$$E_e^F = \sqrt{g_{00}}\mu_e - eV, \tag{3}$$

throughout the entire configuration has been there demonstrated in complete generality. Here g_{00} is the 00 component of the metric tensor, μ_i is the particle chemical potential and units with $\hbar = c = 1$ are adopted. The nuclear interaction is introduced through the exchange of σ, ω, and ρ meson-fields, following the so-called "quantum hadrodynamical model" [6, 7]. The Coulomb potential is denoted by V, e stands for the fundamental charge, σ is an isoscalar meson field that provides the attractive "long" range part of the nuclear force, ω is a massive vector field that provides the repulsive "short" range part of the nuclear force, and ρ is the massive isovector field, that accounts for the isospin contribution. The coupling constants g_s, g_ω and g_ρ and the meson masses m_σ, m_ω and m_ρ are fixed by fitting the experimental properties of nuclei.

The neutron star equilibrium configurations obtained requiring the constancy of the general relativistic Fermi energy for all particle-species are quite different with respect to the ones traditionally constructed, where the assumption of local charge neutrality condition $n_e(r) = n_p(r)$ is adopted. In a recent work [8], it has been shown that such a condition violates the equilibrium conditions of particles given by eqs. (1)–(3). Therefore, instead of local charge neutrality, global charge neutrality $N_e = N_p$, being N_e and N_p the total number of electrons and protons, has been there imposed.

Following the above works [8, 5], we construct here a novel mass-radius relation for neutron stars that satisfy global but not local charge neutrality. For the nuclear model we use the NL3 [9], NL-SH [10], TM1 [11] and TM2 [12] parameterizations. For the crust we select two EoS. The first one assumes a degenerate microscopically uniform electron fluid model, neglecting the Coulomb interactions between the electrons and the nuclear component (Z, A). The second EoS, due to G. Baym *et al.* (BPS) [13], takes into account the Coulomb interaction between point-like nuclei with a uniform fluid of

degenerate electrons, and the nuclear contribution is obtained from experimental data of nuclear masses. We compare and contrast as well the mass and the thickness of the crust obtained with these two different EoS and with the different parameterizations of the σ, ω, and ρ nuclear model.

2. – Equilibrium equations

2˙1. *Equilibrium equations of the core.* – The total Lagrangian density of the system is given by

$$\mathcal{L} = \mathcal{L}_g + \mathcal{L}_f + \mathcal{L}_\sigma + \mathcal{L}_\omega + \mathcal{L}_\rho + \mathcal{L}_\gamma + \mathcal{L}_{int}\,, \tag{4}$$

where the Lagrangian densities for the free-fields are

$$\mathcal{L}_g = -\frac{R}{16\pi G}, \tag{5}$$

$$\mathcal{L}_\gamma = -\frac{1}{16\pi} F_{\mu\nu}F^{\mu\nu}, \tag{6}$$

$$\mathcal{L}_\sigma = \frac{1}{2}\nabla_\mu\sigma\nabla^\mu\sigma - U(\sigma), \tag{7}$$

$$\mathcal{L}_\omega = -\frac{1}{4}\Omega_{\mu\nu}\Omega^{\mu\nu} + \frac{1}{2}m_\omega^2\omega_\mu\omega^\mu, \tag{8}$$

$$\mathcal{L}_\rho = -\frac{1}{4}\mathcal{R}_{\mu\nu}\mathcal{R}^{\mu\nu} + \frac{1}{2}m_\rho^2\rho_\mu\rho^\mu, \tag{9}$$

where $\Omega_{\mu\nu} \equiv \partial_\mu\omega_\nu - \partial_\nu\omega_\mu$, $\mathcal{R}_{\mu\nu} \equiv \partial_\mu\rho_\nu - \partial_\nu\rho_\mu$, $F_{\mu\nu} \equiv \partial_\mu A_\nu - \partial_\nu A_\mu$ are the field strength tensors for the ω^μ, ρ and A^μ fields, respectively, ∇_μ stands for covariant derivative and R is the Ricci scalar. We adopt the Lorenz gauge for the fields A_μ, ω_μ, and ρ_μ. The self-interaction scalar field potential $U(\sigma)$ is a quartic-order polynom for a renormalizable theory (see, *e.g.*, [14]).

The Lagrangian density for the three fermion species is

$$\mathcal{L}_f = \sum_{i=e,N} \bar{\psi}_i \left(i\gamma^\mu D_\mu - m_i\right)\psi_i, \tag{10}$$

where ψ_N is the nucleon isospin doublet, ψ_e is the electronic singlet, m_i states for the mass of each particle-specie and $D_\mu = \partial_\mu + \Gamma_\mu$, being Γ_μ the Dirac spin connections.

The interacting part of the Lagrangian density is, in the minimal-coupling assumption, given by

$$\begin{aligned}\mathcal{L}_{\rm int} = &-g_\sigma\sigma\bar{\psi}_N\psi_N - g_\omega\omega_\mu J^\mu_\omega - g_\rho\rho_\mu J^\mu_\rho \\ &+eA_\mu J^\mu_{\gamma,e} - eA_\mu J^\mu_{\gamma,N},\end{aligned} \tag{11}$$

where J^μ_ω, J^μ_ρ, $J^\mu_{\gamma,e}$ and $J^\mu_{\gamma,N}$ are the conserved currents

The Dirac matrices γ^μ and the isospin Pauli matrices satisfy the Dirac algebra in curved spacetime (see, *e.g.*, [15] for details).

We consider non-rotating neutron stars. Introducing the non-rotating spherically symmetric spacetime metric

$$\mathrm{d}s^2 = e^{\nu(r)}\mathrm{d}t^2 - e^{\lambda(r)}\mathrm{d}r^2 - r^2\mathrm{d}\theta^2 - r^2\sin^2\theta\mathrm{d}\varphi^2, \tag{12}$$

for which the Einstein-Maxwell-Dirac equations read

$$e^{-\lambda(r)}\left(\frac{1}{r^2}-\frac{\lambda'}{r}\right)-\frac{1}{r^2}=-8\pi G T_0^0, \tag{13}$$

$$e^{-\lambda(r)}\left(\frac{1}{r^2}+\frac{\nu'}{r}\right)-\frac{1}{r^2}=-8\pi G T_1^1, \tag{14}$$

$$P'+\frac{\nu'}{2}(\mathcal{E}+P)=-g_\sigma n_s\sigma'-\omega' g_\omega J^0_\omega-\rho' g_\rho J^0_\rho-V' e J^0_{ch}, \tag{15}$$

$$V''+V'\left[\frac{2}{r}-\frac{(\nu'+\lambda')}{2}\right]=-e^\lambda e J^0_{ch}, \tag{16}$$

$$\sigma''+\sigma'\left[\frac{2}{r}+\frac{(\nu'-\lambda')}{2}\right]=e^\lambda\left[\partial_\sigma U(\sigma)+g_s n_s\right], \tag{17}$$

$$\omega''+\omega'\left[\frac{2}{r}-\frac{(\nu'+\lambda')}{2}\right]=-e^\lambda\left[g_\omega J^0_\omega-m^2_\omega\omega\right], \tag{18}$$

$$\rho''+\rho'\left[\frac{2}{r}-\frac{(\nu'+\lambda')}{2}\right]=-e^\lambda\left[g_\rho J^0_\rho-m^2_\rho\rho\right], \tag{19}$$

plus the constancy of the electron Fermi energy and β-equilibrium.

Thanks to the huge number of involved particles ($\sim 10^{57}$), this latter system can be reduced through the mean-field approximation to

$$e^{-\lambda(r)}\left(\frac{1}{r^2}-\frac{1}{r}\frac{\mathrm{d}\lambda}{\mathrm{d}r}\right)-\frac{1}{r^2}=-8\pi G T_0^0, \tag{20}$$

$$e^{-\lambda(r)}\left(\frac{1}{r^2}+\frac{1}{r}\frac{\mathrm{d}\nu}{\mathrm{d}r}\right)-\frac{1}{r^2}=-8\pi G T_1^1, \tag{21}$$

$$V''+\frac{2}{r}V'\left[1-\frac{r(\nu'+\lambda')}{4}\right]=-4\pi e\, e^{\nu/2}e^\lambda(n_p-n_e), \tag{22}$$

$$\frac{\mathrm{d}^2\sigma}{\mathrm{d}r^2}+\frac{\mathrm{d}\sigma}{\mathrm{d}r}\left[\frac{2}{r}-\frac{1}{2}\left(\frac{\mathrm{d}\nu}{\mathrm{d}r}+\frac{\mathrm{d}\lambda}{\mathrm{d}r}\right)\right]=e^\lambda\left[\partial_\sigma U(\sigma)+g_s n_s\right], \tag{23}$$

$$\frac{\mathrm{d}^2\omega}{\mathrm{d}r^2}+\frac{\mathrm{d}\omega}{\mathrm{d}r}\left[\frac{2}{r}-\frac{1}{2}\left(\frac{\mathrm{d}\nu}{\mathrm{d}r}+\frac{\mathrm{d}\lambda}{\mathrm{d}r}\right)\right]=-e^\lambda\left(g_\omega J^0_\omega-m^2_\omega\omega\right), \tag{24}$$

$$\frac{\mathrm{d}^2\rho}{\mathrm{d}r^2}+\frac{\mathrm{d}\rho}{\mathrm{d}r}\left[\frac{2}{r}-\frac{1}{2}\left(\frac{\mathrm{d}\nu}{\mathrm{d}r}+\frac{\mathrm{d}\lambda}{\mathrm{d}r}\right)\right]=-e^\lambda\left(g_\rho J^0_\rho-m^2_\rho\rho\right), \tag{25}$$

$$E^F_e=e^{\nu/2}\mu_e-eV=\text{const}, \tag{26}$$

$$E^F_p=e^{\nu/2}\mu_p+\mathcal{V}_p=\text{const}, \tag{27}$$

$$E^F_n=e^{\nu/2}\mu_n+\mathcal{V}_n=\text{const}, \tag{28}$$

where we have replaced the Tolman-Oppenheimer-Volkov equation with appropriate conservation laws for the generalized particle Fermi energies and the beta equilibrium condition. We have introduced the notation $\omega_0=\omega$, $\rho_0=\rho$, and $A_0=V$ for the time components of the meson fields. Here $\mu_i=\partial\mathcal{E}/\partial n_i=\sqrt{(P^F_i)^2+\tilde{m}^2_i}$ and $n_i=(P^F_i)^3/(3\pi^2)$ are the free chemical potential and number density of the i-species with Fermi momentum P^F_i. The particle effective mass is $\tilde{m}_N=m_N+g_s\sigma$ and $\tilde{m}_e=m_e$ and the effective

TABLE I. – *Selected parameter sets of the σ-ω-ρ model.*

	NL3	NL-SH	TM1	TM2
m_σ (MeV)	508.194	526.059	511.198	526.443
m_ω (MeV)	782.501	783.000	783.000	783.000
m_ρ (MeV)	763.000	763.000	770.000	770.000
g_s	10.2170	10.4440	10.0289	11.4694
g_ω	12.8680	12.9450	12.6139	14.6377
g_ρ	4.4740	4.3830	4.6322	4.6783
g_2 (fm^{-1})	−10.4310	−6.9099	−7.2325	−4.4440
g_3	−28.8850	−15.8337	0.6183	4.6076
c_3	0.0000	0.0000	71.3075	84.5318

potentials $\mathcal{V}_{p,n}$ are given by

$$\mathcal{V}_p = g_\omega\omega + g_\rho\rho + eV\,, \tag{29}$$

$$\mathcal{V}_n = g_\omega\omega - g_\rho\rho\,. \tag{30}$$

Note that in the static case, only the time components of the covariant currents survive, *i.e.* $\langle\bar{\psi}(x)\gamma^i\psi(x)\rangle = 0$. Thus, by taking the expectation values of the conserved currents, we obtain their non-vanishing components

$$J_0^{ch} = n_{ch}u_0 = (n_p - n_e)u_0, \tag{31}$$

$$J_0^{\omega} = n_b u_0 = (n_n + n_p)u_0, \tag{32}$$

$$J_0^{\rho} = n_3 u_0 = (n_p - n_n)u_0, \tag{33}$$

where $n_b = n_p + n_n$ is the baryon number density and $u_0 = \sqrt{g_{00}} = e^{\nu/2}$ is the covariant time component of the four-velocity of the fluid, which satisfies $u^\mu u_\mu = 1$.

In order to integrate the equilibrium equations we need to fix the parameters of the nuclear model, namely, fixing the coupling constants g_s, g_ω and g_ρ, and the meson masses m_σ, m_ω and m_ρ. Conventionally, such constants are fixed by fitting experimental properties of nuclei. Usual experimental properties of ordinary nuclei include saturation density, binding energy per nucleon (or experimental masses), symmetry energy, surface energy, and nuclear incompressibility. In table I we present selected fits of the nuclear parameters.

In fig. 1 we show the results of the integration of the above equations for the NL3, NL-SH, TM1 and TM2 parameterizations of the σ, ω, and ρ model.

2˙2. *Core-crust transition layer.* – Due to the neutrality of the crust (see, *e.g.*, [16]), global charge neutrality must be guaranteed at its edge. The Coulomb potential energy inside the core of the neutron star is found to be $\sim m_\pi c^2$ and related to this there is an internal electric field of order $\sim 10^{-14}E_c$, where $E_c = m_e^2c^3/(e\hbar)$ is the critical field for vacuum polarization. Matching beetwen core and crust is guaranteed by the continuity of all general relativistic particle Fermi energies in the core-crust boundary. As a consequence of such boundary conditions, a core-crust transition surface of thickness $\sim \hbar/(m_e c)$ is developed and in it an overcritical electric field appears [17]. The neutron and proton densities decrease sharply there due to the nuclear surface tension and the

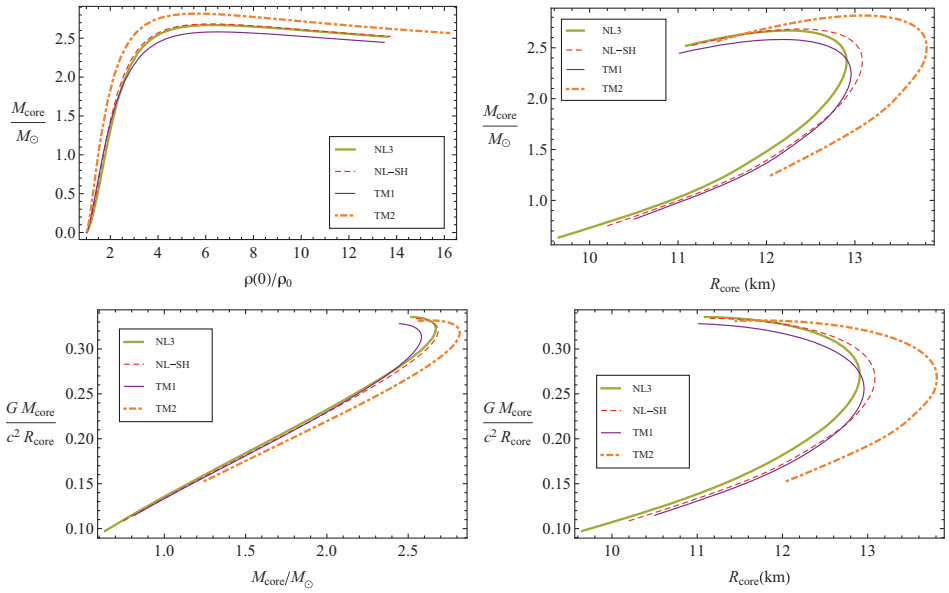

Fig. 1. – Top: Mass-radius relation of neutron star cores for selected parameterizations of the Walecka model. Bottom: Compactness-mass and compactness-radius relations.

electron density also decreases fast and match continuously the electron density at the edge of the crust (see fig. 2 for details). The continuity of the electron Fermi energy puts stringent limits on the density we might have at the edge of the crust: the variation of electron chemical potential at the core-crust boundary $\mu_e(\text{core}) - \mu_e(\text{crust})$ must be necessarily of order $eV \sim m_\pi c^2$. Therefore a suppression of the so-called inner crust of the neutron star is possible if $\mu_e(\text{crust}) \sim \mu_e(\text{core}) - eV \leq 25\,\text{MeV}$, which is approximately the value of the electron chemical potential at the neutron drip point (see, *e.g.*, [13]). We analyze here the structure of neutron star crusts composed only by what is currently known as outer crust, namely a crust with edge density $\sim 4.3 \times 10^{11}\,\text{g/cm}^3$.

2˙3. *Equilibrium equations of the crust.* – Being the crust neutral, its structure equations to be integrated are just the Tolman-Oppenheimer-Volkoff equations

$$\frac{\mathrm{d}P}{\mathrm{d}r} = -\frac{G(\mathcal{E}+P)(m+4\pi r^3 P)}{r^2(1-\frac{2Gm}{r})}\,, \tag{34}$$

$$\frac{\mathrm{d}m}{\mathrm{d}r} = 4\pi r^2 \mathcal{E}, \tag{35}$$

where $m = m(r)$ is the mass enclosed at the radius r.

For a given a core, we integrate the above equations for two different models of the crust. The first one is based on the uniform approximation for the electron fluid. Here the electrons are considered as a fully degenerate free-gas described by Fermi-Dirac statistics. Therefore Coulomb interactions are neglected. Since the electromagnetic interactions are not taken into account, the energy-density is given by $\mathcal{E} = \xi m_n n_e$, where n_e is the number density of electrons and $\xi = A/Z$ is the mean molecular weight per electron. The pressure is the one given by the fluid of degenerate relativistic electrons.

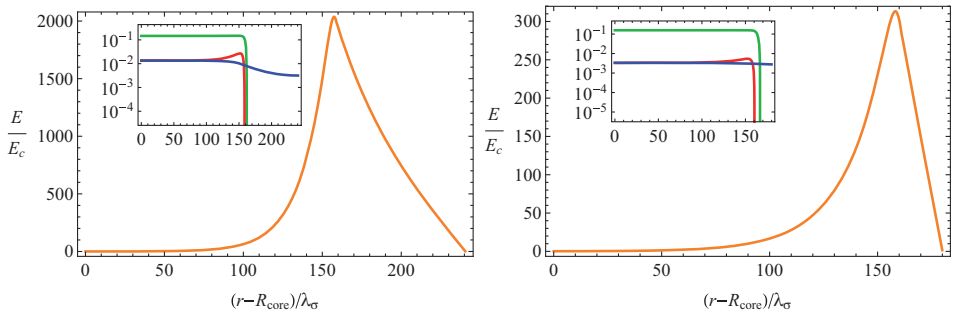

Fig. 2. – (Colour on-line) The electric field in the core-crust transition layer is plotted in units of the critical field E_c for the NL3-model of table I. We show the results for the NL3-model setting $g_\rho \neq 0$ (left plot) and $g_\rho = 0$ (right plot) in order to see the effects of the ρ-meson. The inset plot shows the corresponding core-crust transition layer particle density profiles of neutrons (green), protons (red), and electrons (blue) in units of fm^{-3}. $\lambda_\sigma = \hbar/(m_\sigma c)\,\mathrm{fm}$ denotes the sigma-meson Compton wavelength. Left region: on the proton profile we can see a bump due to Coulomb repulsion while the electron profile decreases. Such a Coulomb effect is indirectly felt also by the neutrons due to the coupled nature of the system of equations. However, the neutron bump is much smaller than the one of protons and it is not appreciable due to the plot scale. Central region: the surface tension due to nuclear interaction produces a sharp decrease of the neutron and proton profiles in a characteristic scale $\sim \lambda_\pi$. Moreover, it can be seen a neutron skin effect, analogous to the one observed in heavy nuclei, which makes the scale of the neutron density falloff slightly larger with respect to the proton one. Right region: smooth decreasing of the electron density similary to the behavior of the electrons surrounding a nucleus in the Thomas-Fermi model.

The second model is based on the EoS by G. Baym, C. Pethick and P. Sutherland (BPS). In this case the crust is divided into Wigner-Size cells; each one of these cells is composed by a point-like nucleus of charge $+Ze$ with A nucleons, surrounded by a uniformly distributed cloud of Z fully degenerate electrons. The contribution of the Coulomb interactions is easily computed thanks to the assumption of microscopic uniformity of the electrons. The sequence of the equilibrium nuclides present at each density between 10^4 and $4.3 \times 10^{11}\,\mathrm{g/cm^3}$ in the BPS EoS is obtained by looking by the nuclear composition that minimizes the energy-density per nucleon. Then in this case the EoS is given by

$$P = P_e + \frac{1}{3} W_L n_N, \tag{36}$$

$$\frac{\mathcal{E}}{n_b} = \frac{W_N + W_L}{A} + \frac{E_e(n_b Z/A)}{n_b}, \tag{37}$$

where $W_N(A, Z)$ is the total energy of an isolated nucleus, including rest mass of the nucleons but not including any electron energy, W_L is the lattice energy (total Coulomb energy) per nucleus, and E_e is the electron energy density.

In figs. 3 we show the mass and the thickness of the crusts obtained from the numerical integration of the structure equations for the two described EoS and for selected cores. It can be seen that we obtain systematically crusts with smaller mass and smaller thickness when Coulomb interactions are taken into account, in line with the results found in [16] in the case of white dwarfs.

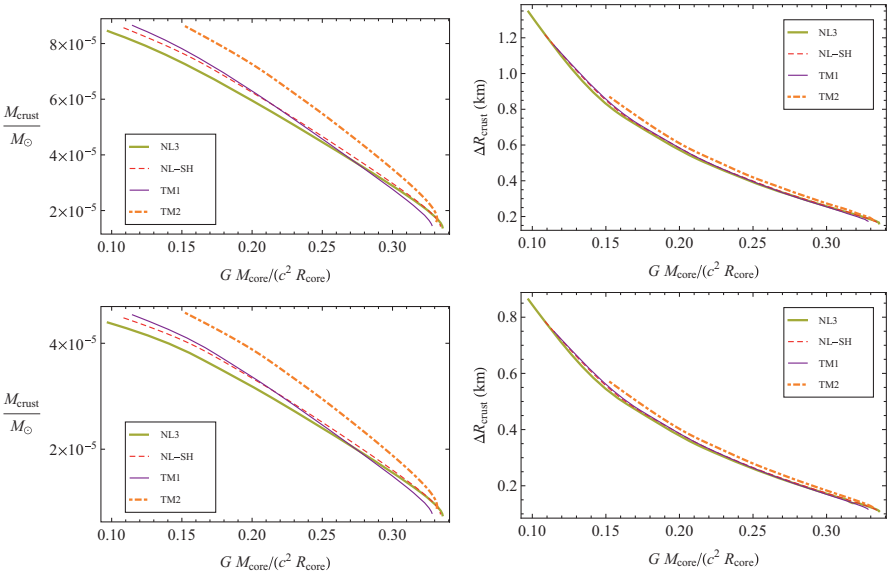

Fig. 3. – Mass (left panels) and thickness (right panels) of the crust for the EoS without Coulomb interaction as a function of the compactness of the core for selected parameterizations of the σ, ω, and ρ model.

The average nuclear composition in the crust can be obtained by calculating the contribution of each nuclear composition to the mass of the crust with respect to the total crust mass. For the two different cores $M_{\rm core} \approx 2.6 M_\odot$, $R_{\rm core} \approx 12.8\,$km and $M_{\rm core} \approx 1.4 M_\odot$, $R_{\rm core} \approx 11.8\,$km (see fig. 4), we obtain as average nuclear composition ${}^{105}_{35}$Br. The corresponding crusts with fixed nuclear composition ${}^{105}_{35}$Br for the two chosen cores are calculated neglecting Coulomb interactions (*i.e.* using the first EoS). The mass and the thickness of these crusts with fixed ${}^{105}_{35}$Br are different with respect to the ones obtained using the full BPS EoS leading to such average nuclear composition. For the two selected examples we obtain that the mass and the thickness of the crust with average ${}^{105}_{35}$Br are, respectively, 18% larger and 5% smaller with respect to those obtained with the corresponding BPS EoS.

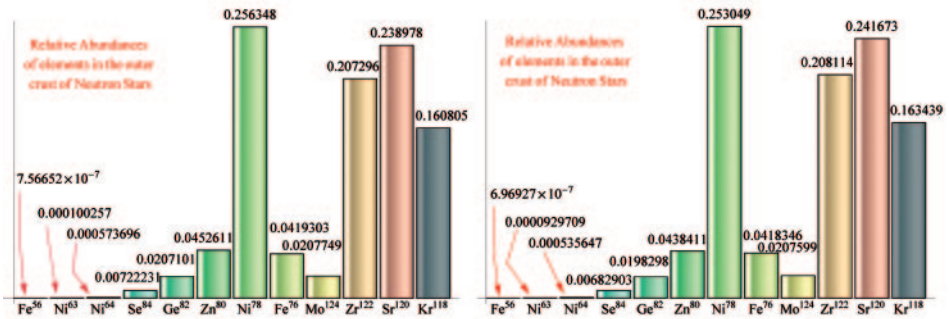

Fig. 4. – Relative abundances of chemical elements in the crust for the two selected cores described in the text.

REFERENCES

[1] Landau L. D. and Lifshitz E. M., *Statistical Physics Part 1* (Pergamon) 1980.
[2] Klein O., *Rev. Mod. Phys.*, **21** (1949) 531.
[3] Kodama T. and Yamada M., *Prog. Theor. Phys.*, **47** (1972) 444.
[4] Olson E. and Bailyn M., *Phys. Rev. D*, **12** (1975) 3030.
[5] Rueda J. A., Ruffini R. and Xue S.-S., *Nucl. Phys. A*, **872** (2011) 286.
[6] Duerr H. P., *Phys. Rev.*, **103** (1956) 469.
[7] Walecka J. D., *Ann. Phys. (N.Y.)*, **83** (1974) 491.
[8] Rotondo M., Rueda J. A, Ruffini R. and Xue S.-S., *Phys. Lett. B*, **701** (2011) 667.
[9] Lalazissis G. A. and König J., *Phys. Rev. C*, **55** (1997) 540.
[10] Sharma M. M., Nagarajan M. A. and Ring P., *Phys. Lett. B*, **312** (1993) 337.
[11] Sugahara Y. and Toki H., *Nucl. Phys. A*, **579** (1994) 557.
[12] Hirata D., Toki H. and Tanihata I., *Nucl. Phys. A*, **589** (1995) 239.
[13] Baym G., Pethick C. and Sutherland P., *Ap. J.*, **170** (1971) 299.
[14] Lee T. D. and Wick G., *Phys. Rev. D*, **9** (1974) 2291.
[15] Lee T. D. and Pang Y., *Phys. Rev. D*, **35** (1987) 3678.
[16] Rotondo M., Rueda J. A., Ruffini R. and Xue S.-S., *Phys. Rev. D*, **84** (2011) 084007.
[17] Belvedere R., Pugliese D., Rueda J. A., Ruffini R. and Xue S.-S., *Nucl. Phys. A.*, **883** (2012) 1.